

<https://doi.org/10.3799/dqkx.2018.153>



拉萨地块中北部尼雄地区早白垩世火山岩的成因及构造意义

苟正彬¹, 刘函¹, 李俊¹, 崔浩杰², 杨洋²

1.中国地质调查局成都地质调查中心, 四川成都 610081

2.成都理工大学地球科学学院, 四川成都 610059

摘要:以往的研究多侧重于拉萨地体中南部,对拉萨地块中北部地区的火山岩浆活动的分布特点、火山岩成因及构造意义关注相对较少,且对该地区中生代火山岩的成因机制存在不同认识。尼雄地区广泛发育的白垩纪火山岩保存了大量青藏高原新生代之前的地质演化信息。岩石学和锆石U-Pb定年研究表明,火山岩类型主要为玄武安山岩、粗面安山岩和流纹岩,其SiO₂含量为55.76%~77.78%,铝饱和指数(A/CNK)为0.89~3.04,属高钾钙碱性-碱钙性-偏铝质-过铝质岩石;其富集Th、U,亏损Nb、Ta等高场强元素,显示出A型花岗质岩石特征;此外,流纹岩具有较高的SiO₂含量和极低的MgO、TiO₂、P₂O₅含量及δEu值,相对亏损Ba、Nb、Ta、Sr和Eu等元素,与高分异的A型流纹岩特征一致。从1个玄武安山岩、1个粗面安山岩和2个流纹岩样品中获得的岩浆锆石U-Pb年龄分别为117 Ma、127 Ma和126~127 Ma,代表了尼雄地区早白垩世火山岩的形成年龄,否定了前人把尼雄地区火山岩全归属为始新世林子宗群年波组或渐新世日贡拉组的认识。综合研究表明,玄武安山岩、粗面安山岩和流纹岩可能为壳幔熔体混合的结果,并伴随着一定的分离结晶作用。它们可能同时受到班公湖-怒江洋壳向南、雅鲁藏布江新特提斯洋壳向北双向俯冲的影响。

关键词:青藏高原;拉萨地块;早白垩世;火山作用;岩石成因;地球化学;地质年代学。

中图分类号: P597

文章编号: 1000-2383(2018)08-2780-15

收稿日期: 2018-03-12

The Petrogenesis and Tectonic Significance of Early Cretaceous Volcanic Rocks in Nixiong Area from the Central and Northern Lhasa Terrane

Gou Zhengbin¹, Liu Han¹, Li Jun¹, Cui Haojie², Yang Yang²

1.Chengdu Center of China Geological Survey, Chengdu 610081, China

2.College of Earth Science, Chengdu University of Technology, Chengdu 610059, China

Abstract: Many studies have been focused on the central and southern Lhasa terrane, but it remains controversial as to the genetic mechanism of the Mesozoic volcanic rocks in the central and northern Lhasa terrane due to less attention paid to the distribution characteristics of volcanic magmatism, the origin of volcanic rocks, and the tectonic significance of the volcanic rocks. Early Cretaceous volcanic rocks are widely exposed in Nixiong area, which record abundant pre-Cenozoic evolutionary geohistory of the Tibetan Plateau. Petrological and zircon U-Pb dating analyses show that the volcanic rocks are mainly composed of basalitic andesite, trachyandesite and rhyolites. They have variable SiO₂ contents ranging from 55.76% to 77.78%, and alumina saturation index (A/CNK) of 0.89~3.04, indicative of high-K calc-alkaline to alkaline-calc and metaluminous to peraluminous. They are characterized by the enrichment of Th and U, and the depletion of HFSEs (such as Nb and Ta), typical of A-type granitoids. In addition, rhyolites show distinct high SiO₂, but low MgO, TiO₂, P₂O₅ and δEu, and display

基金项目:国家自然科学基金项目(Nos.41773026,41303028);中国地质调查局项目(No.DD20160015);四川省基金项目(No.2014JQ0025)。

作者简介:苟正彬(1986—),男,博士研究生,主要从事大陆造山带形成与构造演化研究。ORCID: 0000-0002-0975-3557. E-mail: gzb3792@163.com

引用格式:苟正彬,刘函,李俊,等,2018.拉萨地块中北部尼雄地区早白垩世火山岩的成因及构造意义.地球科学,43(8):2780—2794.

fiercely negative Ba, Nb, Ta, Sr and Eu anomalies, suggesting that they are highly fractionated A-type rocks. LA-ICP-MS U-Pb dating of magmatic zircons from one basalitic andesite, one trachyandesite and two rhyolites samples indicate that they were formed at 117 Ma, 127 Ma and 126–127 Ma, respectively. It is proved that results of previous studies are wrong in that the volcanic rocks in Nixiong area are all Eocene Nianbo Formation of Lingzizhong group or Oligocene Rigongla Formation. In addition, it is found that the basalitic andesite, trachyandesite and rhyolites are likely derived from partial melting of a crust-mantle mixed source, and have experienced significant fractional crystallization. We speculate that the studied rocks have been affected by double subduction of southward subduction of Bangong Co-Nujiang Tethys oceanic crust, and northward subduction of Yalung-Zangbo oceanic crust.

Key words: Tibetan Plateau; Lhasa terrane; Early Cretaceous; volcanism; petrogenesis; geochemistry; geochronology.

0 引言

位于青藏高原南部的拉萨地体(图1a),因其很好地保存了整个造山带的地质演化历史,是研究板块运动和大陆造山作用的理想对象(Yin and Harrison, 2000).然而,以往对拉萨地体的研究多集中在新生代的变形、变质、岩浆活动以及造山作用,其新生代之前的地质演化历史并未得到很好的约束。

青藏高原拉萨地块中广泛发育中生代岩浆岩(康志强等,2009; Ma *et al.*, 2013; Xu *et al.*, 2013),深入研究其成因及构造意义有助于更好地重塑拉萨地体在新生代碰撞之前的地质演化历史.然而,以往的研究多侧重于拉萨地体中南部(常承法和郑锡澜,1973;李才等,2003; Xu *et al.*, 2013),学者们对拉萨地体中北部地区的火山岩浆活动的分布特点、火山岩成因及构造意义关注相对较少,且对该地区中生代火山岩的成因机制也存在不同认识.如新特提斯洋壳北向俯冲(Kapp *et al.*, 2005; Zhang *et al.*, 2012)、班公湖—怒江特提斯洋壳南向俯冲(莫宣学和潘桂棠,2006; 张亮亮等,2010; Zhu

et al., 2011; 张志平等, 2016)、新特提斯洋脊俯冲(管琪等, 2010; Zhang *et al.*, 2010; Meng *et al.*, 2014)以及由于拉萨地体与羌塘地体发生碰撞导致加厚地壳重熔(Harris *et al.*, 1990).因此,要全面分析拉萨地体中生代岩浆作用的动力学机制,还需深入了解冈底斯中北部火山岩蕴含的重要信息.

本文在新近完成的西藏尼雄地区1:5万区域地质调查的基础上,结合新的分析数据,对拉萨地体中北部尼雄地区的早白垩世晚期的中一酸性火山岩进行了岩石学及锆石U-Pb年代学研究,并探讨了其成因及构造意义,为进一步完善拉萨地体在印度与欧亚大陆碰撞之前的构造演化历史提供了重要信息.

1 区域地质概况和样品特征

青藏高原主要由松潘—甘孜杂岩、羌塘地体、拉萨地体和喜马拉雅带4部分组成(Yin and Harrison, 2000),它们之间的界线分别为金沙江、班公湖—怒江和雅鲁藏布江缝合带(图1a).拉萨地体作为冈瓦

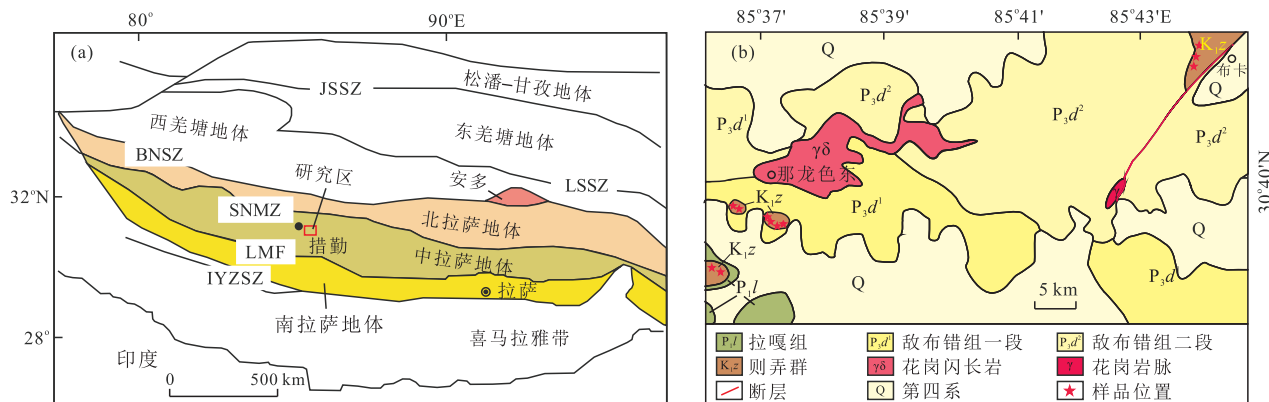


图1 青藏高原地质简图(a)和研究区地质简图(b)

Fig.1 Simplified geological map of the Tibetan Plateau (a) and geological map of the study area (b)

图a据Zhu *et al.*(2008).JSSZ.金沙江缝合带;LSSZ.龙木错—双湖缝合带;BNSZ.班公湖—怒江缝合带;SNMZ.狮泉河—纳木错断裂;LMF.洛巴堆—米拉山断裂;IYZSZ.印度—雅鲁藏布江

纳大陆的北缘,东西延伸近 2 000 km,南北宽约为 300 km.从北至南,拉萨地体被狮泉河—纳木错断裂带和洛巴堆—米拉山断裂带分为北、中和南 3 个亚地体(图 1a; Zhu *et al.*, 2009a).北拉萨亚地体主要由中三叠纪—白垩纪的沉积岩以及大量的白垩纪火山岩和花岗岩组成(Zhu *et al.*, 2009b, 2012),没有前寒武纪的基底岩石(Pan *et al.*, 2004).中拉萨亚地体被认为是前寒武纪结晶基底的典型代表(Pan *et al.*, 2004),主要由前寒武纪一二叠纪的沉积岩(Lin *et al.*, 2013; Xu *et al.*, 2013)和侏罗纪晚期—白垩纪早期的沉积岩及大量的火山岩组成(梁银平等, 2010; Chen *et al.*, 2014).南拉萨亚地体不仅存在少量古老的结晶基底(Dong *et al.*, 2011),还识别出大量的新生地壳(Mo *et al.*, 2008; Chung *et al.*, 2009; Zhu *et al.*, 2011),主要由少量三叠纪—白垩纪早期的火山—沉积岩、白垩纪晚期—第三纪的岩浆岩和第三纪早期的林子宗火山岩组成.

研究区位于措勤县东南方向约 50 km 的尼雄村附近,构造上位于拉萨地体中北部(图 1b).研究区主要出露早二叠世拉嘎组、晚二叠世敌布错组、早白垩世则弄群、晚白垩世花岗闪长岩和第四纪地层.拉嘎组与昂杰组多呈沉积整合关系,则弄群火山岩

角度不整合于早二叠世拉嘎组和晚二叠世敌布错组之上,花岗闪长岩呈近东西向侵位于敌布错组中.研究区则弄群是从早二叠世拉嘎组和晚二叠世敌布错组中解体出来的地层,前人在该区域并未发现则弄群,以往的研究把该区域及邻区所出露的火山岩全归属为始新世林子宗群或渐新世日贡拉组,急需重新厘定.早白垩世则弄群以火山熔岩(安山岩和流纹岩)为主,相伴发育有火山碎屑岩(英安质一流纹质晶屑凝灰岩、熔结凝灰岩、凝灰熔岩)和碎屑岩(粗—细砂岩).本文所研究的火山岩包括流纹岩、粗面安山岩和玄武安山岩.玄武安山岩呈斑状结构,斑晶为斜长石和暗色矿物假象,粒度一般为 0.4~1.5 mm,零散分布;基质呈玻基交织结构,由长石、石英、暗色矿物假象组成,长石以斜长石为主,粒径一般 <0.2 mm,似交织状分布,石英呈他形粒状,零散分布于长石空隙间,暗色矿物常被黑云母—绿泥石、碳酸盐等交代呈假象,填隙于上述长石间(图 2a).粗面英安岩为斑状结构,斑晶多为斜长石,基质为斜长石、石英及黑云母,斜长石无规则排列,可见双晶及环带结构(图 2b).流纹岩为斑状结构,斑晶为石英和斜长石,石英多被熔蚀,局部可见港湾状结构,基质由细小的长石、石英及玻璃质组成(图 2c,2d).

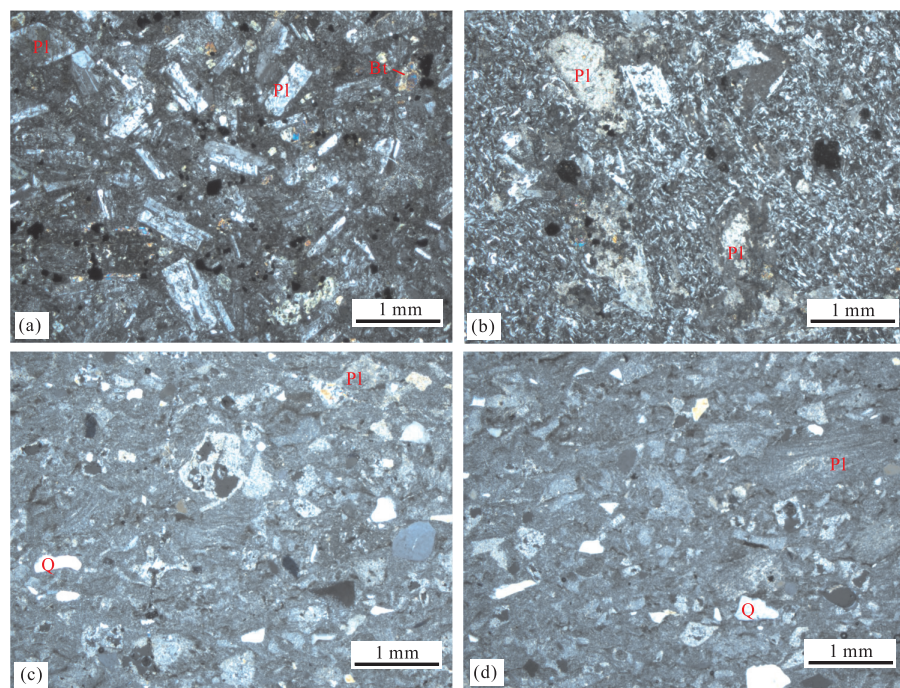


图 2 玄武安山岩(a)、粗面安山岩(b)和流纹岩(c,d)样品显微镜下照片

Fig.2 Photomicrographs of the basalitic andesite (a), trachyandesite (b) and rhyolite (c,d) samples
Q.石英;Pl.斜长石;Bt.黑云母

2 分析方法

锆石 U-Pb 定年在中国地质大学(武汉)地质过程与矿产资源国家重点实验室完成。测试仪器为 LA-ICP-MS, 激光剥蚀系统为 GeoLas 2005, ICP-MS 等离子质谱仪为 Agilent 7500a, 激光剥蚀深度为 20~40 μm, 剥蚀斑束直径为 32 μm。详细的仪器操作条件见 Liu *et al.* (2010), 采用软件 ICPMSDataCal 对分析数据进行离线处理。使用 ISOPLOT 软件对同位素数据结果进行处理 (Ludwig, 2003)。

在野外地质研究的基础上, 笔者挑选无脉体、无蚀变(或弱蚀变, 烧失量<4%) 的样品进行研究。将样品无污染地粉碎至 200 目。全岩化学成分分析在国家地质实验测试中心完成。主量元素的测试分析采用 X-ray 荧光光谱法(Rigaku-3080), 分析精度优于 0.5%。微量元素 Nb、Zr、Cr、V、Sr、Zn、Ba、Ni、Y 和 Rb 使用与测试主量元素不同的 XRF 设备(Rigaku-2100)进行分析, 分析精度优于 3%~5%。其他稀土元素和微量元素使用电感耦合等离子体质谱仪进行分析测试, 当元素含量大于 1×10^{-6} 时, 分析精度优于 1%~5%; 当元素含量小于 1×10^{-6} 时,

分析精度优于 5%~10%。

3 锆石 U-Pb 定年

玄武安山岩中的锆石具有类似的外形特征, 呈自形长柱状, 长为 80~150 μm, 长宽比为 1:1~2.5:1。阴极发光图像显示这些锆石普遍具有振荡环带(图 3a), 且 Th/U 比值为 0.98~2.83(表 1), 说明锆石属岩浆成因(Hoskin and Schaltegger, 2003; Rubatto and Scambelluri, 2003; 吴元保和郑永飞, 2004)。样品 D1651-N1 的 11 个分析点获得了近一致的 117.1 ± 1.3 Ma 的锆石 U-Pb 谱和年龄(图 3a)。

粗面安山岩中的锆石呈自形短柱—长柱状, 长为 50~150 μm, 长宽比为 1:1~2:1。这些锆石具有典型的韵律环带(图 3b), Th/U 比值为 1.00~1.49(表 1), 显示出岩浆成因锆石的特征。该样品的 12 个分析点获得了近一致的 127.5 ± 2.4 Ma 的锆石 U-Pb 年龄(图 3b)。

流纹岩中的锆石呈自形短柱—长柱状, 长为 100~200 μm, 长宽比为 1:1~3.5:1, 韵律环带明显(图 3c, 3d), Th/U 比值大(0.75~1.79; 表 1), 代

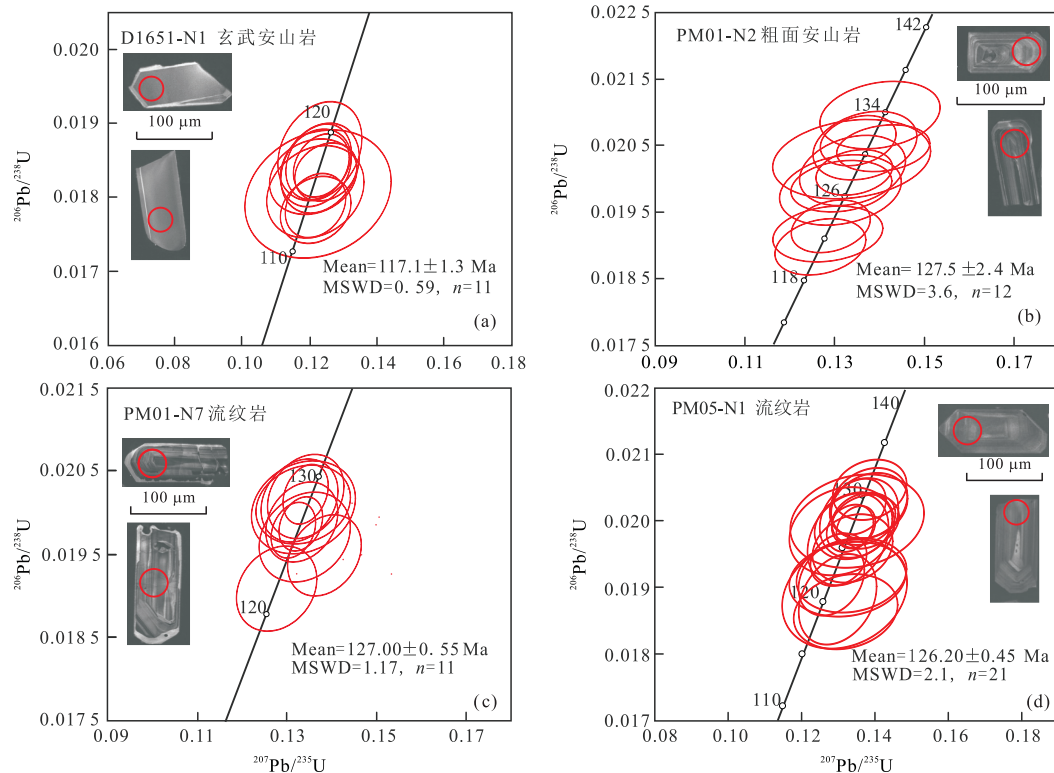


图 3 早白垩世火山岩锆石 U-Pb 谱和图及代表性锆石阴极发光图像

Fig.3 Zircon U-Pb concordia plots of the Early Cretaceous volcanic rocks, showing CL images of the typical zircon grains
圆圈为 U-Pb 年龄分析点

表 1 玄武安山岩、粗面安山岩与流纹岩 LA-ICPMS 锆石 U-Pb 定年结果
Table 1 LA-ICPMS zircon U-Pb data of the basaltic andesite, trachyandesite and rhyolite

| 样品 | 元素含量(10^{-6}) | | | 同位素比值 | | | 年龄(Ma) | | | | | |
|-----------------------|-------------------|-------|-------|-------|-----------------------------------|-----------|----------------------------------|-----------|----------------------------------|-----------|----------------------------------|-----------|
| | Pb | Th | U | Th/U | $^{207}\text{Pb}/^{206}\text{Pb}$ | 1σ | $^{206}\text{Pb}/^{238}\text{U}$ | 1σ | $^{207}\text{Pb}/^{235}\text{U}$ | 1σ | $^{206}\text{Pb}/^{238}\text{U}$ | 1σ |
| D1651-N1 玄武安山岩 | | | | | | | | | | | | |
| D1651-N1-05 | 49 | 544 | 290 | 1.88 | 0.048 0 | 0.007 6 | 0.123 3 | 0.019 9 | 0.018 1 | 0.000 6 | 98 | 337.0 |
| D1651-N1-06 | 63 | 764 | 644 | 1.19 | 0.050 7 | 0.004 7 | 0.124 1 | 0.010 6 | 0.018 5 | 0.000 4 | 228 | 203.7 |
| D1651-N1-07 | 86 | 1 131 | 990 | 1.14 | 0.050 6 | 0.005 6 | 0.121 3 | 0.011 9 | 0.018 4 | 0.000 3 | 220 | 237.0 |
| D1651-N1-08 | 129 | 1 599 | 1 627 | 0.98 | 0.049 6 | 0.003 9 | 0.123 5 | 0.008 9 | 0.018 6 | 0.000 3 | 176 | 174.0 |
| D1651-N1-12 | 222 | 2 999 | 1 974 | 1.52 | 0.049 0 | 0.003 2 | 0.124 6 | 0.007 6 | 0.018 5 | 0.000 3 | 146 | 153.7 |
| D1651-N1-13 | 185 | 2 493 | 882 | 2.83 | 0.049 7 | 0.003 4 | 0.126 5 | 0.008 4 | 0.018 4 | 0.000 3 | 189 | 167.6 |
| D1651-N1-14 | 96 | 1 120 | 482 | 2.32 | 0.048 0 | 0.004 0 | 0.122 3 | 0.009 6 | 0.018 5 | 0.000 3 | 98 | 185.2 |
| D1651-N1-15 | 32 | 382 | 320 | 1.19 | 0.052 6 | 0.005 4 | 0.124 1 | 0.011 4 | 0.018 7 | 0.000 4 | 322 | 233.3 |
| D1651-N1-17 | 81 | 1 048 | 482 | 2.17 | 0.050 7 | 0.004 2 | 0.122 3 | 0.009 6 | 0.017 9 | 0.000 3 | 233 | 194.4 |
| D1651-N1-18 | 51 | 629 | 316 | 1.99 | 0.051 7 | 0.005 7 | 0.122 2 | 0.013 2 | 0.018 2 | 0.000 4 | 272 | 237.0 |
| D1651-N1-19 | 143 | 1 904 | 1 302 | 1.46 | 0.050 0 | 0.003 5 | 0.122 2 | 0.008 2 | 0.018 0 | 0.000 3 | 195 | 164.8 |
| PM01-N2 粗面安山岩 | | | | | | | | | | | | |
| PM01-N2-01 | 76 | 976 | 787 | 1.24 | 0.051 3 | 0.003 5 | 0.142 9 | 0.009 0 | 0.019 5 | 0.000 3 | 257 | 161.1 |
| PM01-N2-02 | 108 | 1 414 | 1 329 | 1.06 | 0.048 1 | 0.002 2 | 0.135 9 | 0.005 5 | 0.020 2 | 0.000 2 | 102 | 107.4 |
| PM01-N2-05 | 67 | 939 | 683 | 1.38 | 0.047 8 | 0.002 1 | 0.131 3 | 0.005 5 | 0.019 8 | 0.000 2 | 87 | 100.0 |
| PM01-N2-06 | 129 | 1 663 | 1 460 | 1.14 | 0.045 6 | 0.003 4 | 0.133 6 | 0.009 4 | 0.020 2 | 0.000 3 | 127 | 8.4 |
| PM01-N2-07 | 67 | 868 | 768 | 1.13 | 0.043 0 | 0.004 4 | 0.135 1 | 0.012 8 | 0.020 1 | 0.000 4 | 129 | 11.4 |
| PM01-N2-08 | 95 | 1 223 | 1 140 | 1.07 | 0.048 4 | 0.003 5 | 0.134 5 | 0.008 8 | 0.019 9 | 0.000 3 | 120 | 159.2 |
| PM01-N2-09 | 122 | 1 665 | 1 118 | 1.49 | 0.047 9 | 0.003 8 | 0.125 1 | 0.009 9 | 0.019 1 | 0.000 3 | 95 | 238.9 |
| PM01-N2-10 | 76 | 1 000 | 893 | 1.12 | 0.045 2 | 0.004 1 | 0.135 6 | 0.011 2 | 0.019 7 | 0.000 4 | 129 | 10.0 |
| PM01-N2-11 | 52 | 645 | 643 | 1.00 | 0.049 0 | 0.002 1 | 0.134 1 | 0.005 4 | 0.019 9 | 0.000 2 | 146 | 100.0 |
| PM01-N2-12 | 139 | 1 850 | 1 787 | 1.04 | 0.048 0 | 0.003 6 | 0.135 9 | 0.009 4 | 0.020 2 | 0.000 3 | 102 | 231.5 |
| PM01-N2-17 | 108 | 1 459 | 1 013 | 1.44 | 0.046 9 | 0.004 8 | 0.135 0 | 0.011 6 | 0.020 1 | 0.000 3 | 56 | 220.3 |
| PM01-N7 流纹岩 | | | | | | | | | | | | |
| PM01-N7-01 | 73 | 970 | 624 | 1.55 | 0.049 1 | 0.002 4 | 0.129 8 | 0.006 5 | 0.019 3 | 0.000 3 | 154 | 116.7 |
| PM01-N7-02 | 56 | 675 | 655 | 1.03 | 0.047 7 | 0.003 6 | 0.135 2 | 0.008 8 | 0.020 1 | 0.000 3 | 83 | 170.3 |
| PM01-N7-03 | 60 | 769 | 670 | 1.15 | 0.044 9 | 0.003 6 | 0.132 2 | 0.010 1 | 0.019 8 | 0.000 3 | 126 | 9.1 |
| PM01-N7-05 | 61 | 760 | 662 | 1.15 | 0.045 5 | 0.003 4 | 0.142 1 | 0.010 0 | 0.021 0 | 0.000 3 | 135 | 8.9 |
| PM01-N7-09 | 45 | 533 | 464 | 1.15 | 0.050 2 | 0.002 6 | 0.143 0 | 0.007 7 | 0.020 5 | 0.000 2 | 206 | 122.2 |

续表1

| 样品 | 元素含量(10^{-6}) | | Th/U | $^{207}\text{Pb}/^{206}\text{Pb}$ | 1σ | 同位素比值 | | $^{206}\text{Pb}/^{238}\text{U}$ | 1σ | $^{207}\text{Pb}/^{235}\text{U}$ | 1σ | $^{206}\text{Pb}/^{238}\text{U}$ | 1σ | 年龄(Ma) | | |
|------------|-------------------|-------|----------------------|-----------------------------------|-----------|-----------------------------------|----------------------------------|----------------------------------|-----------|----------------------------------|-----------|----------------------------------|-----------|--------|-----|-----|
| | Pb | Th | | | | $^{207}\text{Pb}/^{206}\text{Pb}$ | $^{206}\text{Pb}/^{238}\text{U}$ | | | | | | | | | |
| 流纹岩 | | | | | | | | | | | | | | | | |
| PM01-N7 | 74 | 975 | 857 | 1.14 | 0.046 4 | 0.005 2 | 0.135 0 | 0.013 1 | 0.020 3 | 0.000 4 | 17 | 316.6 | 129 | 11.7 | 129 | 2.5 |
| PM01-N7-11 | 193 | 2 373 | 2 304 | 1.03 | 0.047 9 | 0.003 8 | 0.129 0 | 0.009 1 | 0.019 2 | 0.000 3 | 100 | 233.3 | 123 | 8.2 | 122 | 1.8 |
| PM01-N7-14 | 50 | 603 | 651 | 0.93 | 0.048 4 | 0.003 1 | 0.132 4 | 0.008 4 | 0.019 9 | 0.000 3 | 117 | 144.4 | 126 | 7.5 | 127 | 1.6 |
| PM01-N7-15 | 107 | 1 254 | 903 | 1.39 | 0.048 7 | 0.002 4 | 0.135 7 | 0.006 3 | 0.020 1 | 0.000 2 | 200 | 119.4 | 129 | 5.7 | 128 | 1.4 |
| PM01-N7-16 | 11 | 159 | 181 | 0.88 | 0.047 6 | 0.002 4 | 0.136 7 | 0.006 3 | 0.020 6 | 0.000 2 | 83 | 114.8 | 130 | 5.6 | 131 | 1.6 |
| PM01-N7-17 | 101 | 1 280 | 1 008 | 1.27 | 0.048 5 | 0.003 1 | 0.127 2 | 0.007 5 | 0.019 0 | 0.000 3 | 124 | 209.2 | 122 | 6.8 | 121 | 1.8 |
| PM01-N7-19 | 154 | 2 083 | 1 706 | 1.22 | 0.046 6 | 0.003 3 | 0.138 4 | 0.008 6 | 0.020 5 | 0.000 3 | 33 | 157.4 | 132 | 7.7 | 131 | 2.1 |
| PM05-N1 | 流纹岩 | | 流纹岩 | | 流纹岩 | | 流纹岩 | | 流纹岩 | | 流纹岩 | | 流纹岩 | | 流纹岩 | |
| PM05-N1-01 | 58 | 559 | 684 | 0.82 | 0.047 2 | 0.004 0 | 0.133 0 | 0.010 6 | 0.019 9 | 0.000 3 | 61 | 194.4 | 127 | 9.5 | 127 | 2.1 |
| PM05-N1-02 | 77 | 753 | 761 | 0.99 | 0.047 7 | 0.003 7 | 0.139 7 | 0.010 1 | 0.020 5 | 0.000 3 | 87 | 174.0 | 133 | 9.0 | 131 | 1.9 |
| PM05-N1-03 | 22 | 229 | 305 | 0.75 | 0.038 7 | 0.006 0 | 0.130 5 | 0.015 9 | 0.019 1 | 0.000 4 | 125 | 14.3 | 122 | 2.3 | | |
| PM05-N1-04 | 40 | 379 | 440 | 0.86 | 0.045 7 | 0.004 1 | 0.135 3 | 0.010 7 | 0.020 0 | 0.000 4 | 129 | 9.6 | 128 | 2.5 | | |
| PM05-N1-05 | 130 | 1 453 | 810 | 1.79 | 0.049 4 | 0.003 3 | 0.137 2 | 0.008 7 | 0.020 0 | 0.000 3 | 169 | 38.9 | 131 | 7.7 | 128 | 1.6 |
| PM05-N1-06 | 49 | 550 | 476 | 1.16 | 0.045 5 | 0.003 9 | 0.132 6 | 0.010 9 | 0.019 6 | 0.000 3 | 126 | 9.8 | 125 | 2.1 | | |
| PM05-N1-07 | 28 | 298 | 270 | 1.10 | 0.044 1 | 0.006 8 | 0.134 5 | 0.018 3 | 0.020 0 | 0.000 5 | 128 | 16.3 | 128 | 2.9 | | |
| PM05-N1-08 | 65 | 671 | 587 | 1.14 | 0.047 2 | 0.004 2 | 0.139 3 | 0.010 6 | 0.020 3 | 0.000 3 | 58 | 200.0 | 132 | 9.4 | 129 | 2.2 |
| PM05-N1-09 | 54 | 565 | 468 | 1.21 | 0.046 5 | 0.004 3 | 0.130 7 | 0.011 1 | 0.019 7 | 0.000 5 | 33 | 201.8 | 125 | 9.9 | 126 | 2.9 |
| PM05-N1-10 | 32 | 287 | 299 | 0.96 | 0.045 5 | 0.006 0 | 0.128 2 | 0.014 3 | 0.019 8 | 0.000 4 | 122 | 12.9 | 127 | 2.8 | | |
| PM05-N1-11 | 112 | 1 239 | 961 | 1.29 | 0.048 1 | 0.002 9 | 0.134 8 | 0.007 7 | 0.020 2 | 0.000 3 | 106 | 133.3 | 128 | 6.9 | 129 | 1.7 |
| PM05-N1-12 | 44 | 461 | 474 | 0.97 | 0.048 6 | 0.004 1 | 0.139 6 | 0.010 4 | 0.020 2 | 0.000 3 | 132 | 185.2 | 133 | 9.3 | 129 | 2.0 |
| PM05-N1-13 | 33 | 325 | 322 | 1.01 | 0.044 0 | 0.005 8 | 0.132 2 | 0.015 0 | 0.019 2 | 0.000 4 | 126 | 13.5 | 122 | 2.3 | | |
| PM05-N1-14 | 192 | 2 144 | 1 621 | 1.32 | 0.048 8 | 0.001 9 | 0.134 0 | 0.005 3 | 0.019 9 | 0.000 2 | 200 | 92.6 | 128 | 4.8 | 127 | 1.3 |
| PM05-N1-15 | 82 | 863 | 850 | 1.02 | 0.047 0 | 0.002 9 | 0.126 8 | 0.007 7 | 0.019 4 | 0.000 3 | 56 | 131.5 | 121 | 6.9 | 124 | 1.6 |
| PM05-N1-16 | 28 | 310 | 274 | 1.13 | 0.044 5 | 0.006 8 | 0.129 3 | 0.017 1 | 0.018 9 | 0.000 5 | 123 | 15.3 | 121 | 3.4 | | |
| PM05-N1-18 | 78 | 685 | 683 | 1.27 | 0.047 4 | 0.004 2 | 0.126 4 | 0.010 6 | 0.018 8 | 0.000 4 | 78 | 187.0 | 121 | 9.6 | 120 | 2.8 |
| PM05-N1-19 | 62 | 676 | 598 | 1.13 | 0.048 8 | 0.005 9 | 0.129 7 | 0.014 2 | 0.018 6 | 0.000 4 | 139 | 259.2 | 124 | 12.8 | 119 | 2.3 |
| PM05-N1-20 | 111 | 1 136 | 1 209 | 0.94 | 0.047 8 | 0.002 4 | 0.131 6 | 0.006 4 | 0.019 9 | 0.000 2 | 100 | 111.1 | 125 | 5.7 | 127 | 1.5 |
| PM05-N1-21 | 236 | 2 898 | 2 941 | 0.99 | 0.049 5 | 0.003 5 | 0.137 9 | 0.009 2 | 0.020 0 | 0.000 3 | 169 | 159.2 | 131 | 8.2 | 128 | 1.7 |
| PM05-N1-22 | 124 | 1 316 | 1 524 | 0.86 | 0.046 7 | 0.003 3 | 0.123 9 | 0.009 0 | 0.019 1 | 0.000 4 | 35 | 159.2 | 119 | 8.1 | 122 | 2.3 |

表岩浆结晶成因。2 个样品获得的锆石 U-Pb 年龄近于一致, 分别为 127.00 ± 0.55 Ma 和 126.20 ± 0.45 Ma(图 3c,3d)。

4 岩石化学

考虑到本文中的 2 件玄武安山岩、4 件粗面安山岩和 5 件流纹岩样品具有相对较高的 LOI、CO₂ 和 H₂O 含量(表 2), 可能遭受了一定的弱蚀变作用, 笔者在对这些样品进行岩石分类和成因研究时, 先将主量元素含量去除 CO₂ 和 H₂O 后再进行换算, 同时尽量避免使用易活动元素(如 Ba、Sr、Na、K 等)。岩相学研究和岩石分类图解结果显示, 研究区早白垩世火山岩应为玄武安山岩、粗面安山岩和流纹岩(图 4a,4b)。

玄武安山岩的 SiO₂ 含量为 55.79%~56.15%, TiO₂ 为 0.89%~0.90%, Al₂O₃ 为 16.86%~16.97%, MgO 为 3.58%~3.82%, Cr 含量为 20.2×10^{-6} ~ 28.3×10^{-6} , Ni 含量为 8.4×10^{-6} ~ 12.3×10^{-6} 以及 Mg[#] 为 47.21~48.36(表 2), 主体为高钾钙碱性岩石, 小部分为中钾钙碱性岩石(图 5)。在微量元素原始地幔标准化蛛网图中, 玄武安山岩富集不相容元素 Th、U 而亏损 Nb、Ta(图 6a)。在稀土元素球粒陨石标准化配分曲线上, 玄武安山岩表现为较缓的右倾曲线配分模式, 轻、重稀土元素分馏程度一般, (La/Yb)_N 比值为 6.51~6.59, Eu/Eu* 介于 0.82~0.86, 弱的负 Eu 异常(图 6b)。

粗面安山岩具有较稳定的 SiO₂、TiO₂ 和 Al₂O₃ 含量, 分别为 55.76%~57.82%、1.21%~1.41%、17.14%~17.86%, 具有较低的 MnO

(0.14%~0.18%)、Ni(1.8×10^{-6} ~ 3.5×10^{-6}) 和 Cr (1.2×10^{-6} ~ 5.0×10^{-6}) 含量及 Mg[#] 值(38.49~49.26), 较高的 K₂O(1.50%~2.16%) 和 Zr 含量 (170×10^{-6} ~ 187×10^{-6})。岩石的铝饱和指数(A/CNK)为 1.00~1.27, 属偏铝—过铝质岩石。粗面安山岩主要为镁质(图 7a)和钙性—碱钙性岩石(图 7b)。如图 6a 所示, 粗面安山岩表现为富集 Rb、Th、U、Nd、Pb、Zr、Hf 等元素, 亏损 Nb、Ta 等高场强元素; 图 6b 中该岩石的轻、重稀土元素分馏明显 ((La/Yb)_N=5.21~5.53), 表现为富集轻稀土、重稀土相对平坦、弱的负 Eu 异常的特点(δEu 为 0.83~0.87)。

流纹岩具有较高的 SiO₂(71.36%~78.78%)、K₂O(2.18%~4.28%) 含量及高的 K₂O/Na₂O 值(0.61~47.56) 和 铝 饱 和 指 数 (A/CNK 为 1.40~3.14), 为过铝质岩石。流纹岩样品介于铁质—镁质之间(图 7a), 属钙碱性—碱钙性岩石(图 7b)。如图 6a 所示, 流纹岩富集 Rb、Th、U、Pb、Nd、Hf 等元素, 且具有强烈的 Ba、Sr、Nb、Ta 和 Eu 负异常的特征; 如图 6b 所示, 流纹岩轻、重稀土元素分馏明显 ((La/Yb)_N=7.43~12.52), 具有明显的负 Eu 异常(δEu 为 0.33~0.75)。

5 讨论

5.1 拉萨地块中北部的白垩纪火山作用

前人将尼雄地区及邻区出露的火山岩划分为渐新世日贡拉组(E₃r)或者始新世波组(E₂n), 而本次研究表明研究区则弄群火山岩获得了 117.1~127.5 Ma 的锆石 U-Pb 年龄, 形成于早白垩世。且则

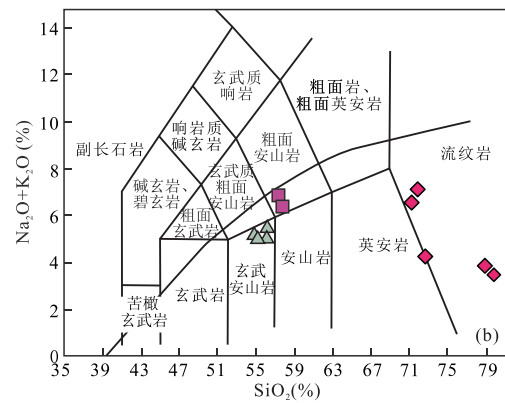
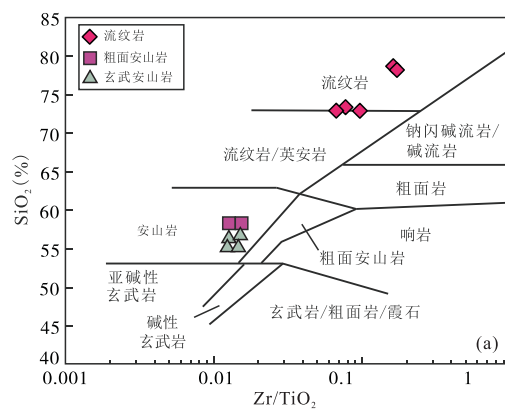


图 4 早白垩世火山岩 SiO₂—Zr/TiO₂(a) 和 (Na₂O+K₂O)—SiO₂ 图解(b)

Fig.4 SiO₂—Zr/TiO₂(a) and (Na₂O+K₂O)—SiO₂ (b) diagrams of the Early Cretaceous volcanic rocks

图 a 据 Winchester and Floyd (1977); 图 b 据 Frost et al. (2001)

表2 早白垩世火山岩全岩主量(%)、微量元素(10^{-6})和稀土元素(10^{-6})分析结果Table 2 Major elements (%), trace elements (10^{-6}) and rare earth elements (10^{-6}) results of Early Cretaceous volcanic rocks

| 岩性 样品 | 玄武安山岩 | | | 粗面安山岩 | | | | 流纹岩 | | | |
|--------------------------------|----------|----------|---------|---------|---------|----------|---------|---------|---------|---------|---------|
| | D1651-H1 | D1651-H2 | PM01-H6 | PM01-H8 | PM01-H7 | PM01-H12 | PM01-H1 | PM01-H2 | PM05-H1 | PM05-H2 | PM05-H3 |
| SiO ₂ | 55.79 | 56.15 | 56.48 | 55.76 | 57.82 | 57.44 | 71.36 | 71.96 | 72.57 | 78.37 | 78.78 |
| TiO ₂ | 0.90 | 0.89 | 1.41 | 1.36 | 1.21 | 1.34 | 0.35 | 0.36 | 0.32 | 0.11 | 0.14 |
| Al ₂ O ₃ | 16.97 | 16.86 | 17.44 | 17.86 | 17.16 | 17.14 | 15.34 | 15.48 | 15.96 | 12.93 | 13.51 |
| Fe ₂ O ₃ | 8.08 | 7.93 | 8.17 | 8.04 | 7.47 | 7.29 | 2.14 | 2.22 | 2.90 | 2.04 | 0.91 |
| MnO | 0.13 | 0.14 | 0.16 | 0.17 | 0.14 | 0.18 | 0.13 | 0.13 | 0.01 | 0.01 | 0.01 |
| MgO | 3.82 | 3.58 | 3.23 | 3.94 | 2.36 | 2.88 | 0.66 | 0.61 | 0.28 | 0.26 | 0.33 |
| CaO | 5.54 | 6.20 | 3.44 | 3.40 | 4.35 | 3.11 | 1.06 | 0.48 | 0.10 | 0.06 | 0.10 |
| Na ₂ O | 3.72 | 3.56 | 3.94 | 3.38 | 4.62 | 4.49 | 3.90 | 4.42 | 0.16 | 0.08 | 0.12 |
| K ₂ O | 1.82 | 1.66 | 1.87 | 2.11 | 1.50 | 2.16 | 2.38 | 2.18 | 4.28 | 3.95 | 3.76 |
| P ₂ O ₅ | 0.20 | 0.22 | 0.36 | 0.36 | 0.37 | 0.37 | 0.09 | 0.09 | 0.07 | 0.06 | 0.03 |
| LOI | 2.94 | 2.70 | 3.40 | 3.54 | 2.92 | 3.45 | 2.54 | 2.02 | 3.26 | 2.09 | 2.26 |
| Total | 99.91 | 99.89 | 99.90 | 99.92 | 99.92 | 99.85 | 99.95 | 99.95 | 99.90 | 99.96 | 99.94 |
| K+Na | 5.54 | 5.22 | 5.81 | 5.49 | 6.12 | 6.65 | 6.28 | 6.60 | 4.44 | 4.03 | 3.88 |
| K/Na | 0.49 | 0.47 | 0.47 | 0.62 | 0.32 | 0.48 | 0.61 | 0.49 | 26.75 | 47.59 | 31.33 |
| A/CNK | 0.93 | 0.89 | 1.18 | 1.27 | 1.00 | 1.11 | 1.40 | 1.47 | 3.14 | 2.86 | 3.04 |
| A/NK | 2.10 | 2.20 | 2.05 | 2.28 | 1.86 | 1.76 | 1.71 | 1.61 | 3.26 | 2.93 | 3.17 |
| Mg [#] | 48.36 | 47.21 | 43.92 | 49.26 | 38.49 | 43.90 | 37.92 | 35.25 | 16.06 | 20.16 | 41.80 |
| La | 28.3 | 28.4 | 32.2 | 29.2 | 32.0 | 31.7 | 44.1 | 41.8 | 55.2 | 46.9 | 67.1 |
| Ce | 54.1 | 54.8 | 64.4 | 60.3 | 65.5 | 62.2 | 83.5 | 78.2 | 115.0 | 91.5 | 124 |
| Pr | 6.3 | 6.3 | 8.2 | 7.5 | 8.0 | 7.9 | 9.3 | 8.9 | 12.5 | 11.3 | 14.6 |
| Nd | 24.4 | 24.3 | 33.3 | 30.2 | 32.4 | 32.5 | 33.7 | 31.9 | 47.0 | 42.2 | 52.5 |
| Sm | 5.0 | 5.0 | 7.3 | 6.6 | 7.1 | 7.3 | 6.1 | 5.8 | 9.6 | 8.5 | 9.7 |
| Eu | 1.4 | 1.3 | 2.1 | 1.9 | 1.9 | 2.1 | 1.2 | 1.3 | 1.4 | 0.9 | 1.2 |
| Gd | 5.2 | 5.1 | 7.8 | 7.0 | 7.2 | 7.8 | 5.3 | 5.3 | 9.1 | 7.9 | 8.2 |
| Tb | 0.8 | 0.8 | 1.2 | 1.1 | 1.1 | 1.2 | 0.8 | 0.8 | 1.4 | 1.2 | 1.2 |
| Dy | 5.2 | 5.2 | 7.6 | 6.7 | 7.1 | 7.3 | 5.4 | 5.3 | 8.6 | 7.6 | 7.1 |
| Ho | 1.0 | 1.0 | 1.5 | 1.3 | 1.4 | 1.5 | 1.1 | 1.1 | 1.7 | 1.5 | 1.4 |
| Er | 3.2 | 3.1 | 4.6 | 4.0 | 4.3 | 4.3 | 3.5 | 3.6 | 5.1 | 4.6 | 4.0 |
| Tm | 0.5 | 0.5 | 0.7 | 0.6 | 0.6 | 0.6 | 0.5 | 0.6 | 0.8 | 0.7 | 0.6 |
| Yb | 3.1 | 3.0 | 4.4 | 3.8 | 4.1 | 4.2 | 3.9 | 3.9 | 5.2 | 4.4 | 3.8 |
| Lu | 0.5 | 0.4 | 0.6 | 0.6 | 0.6 | 0.6 | 0.6 | 0.6 | 0.8 | 0.6 | 0.5 |
| Σ REE | 138.8 | 139.3 | 175.8 | 160.7 | 173.2 | 171.2 | 199 | 189 | 273 | 230 | 296 |
| Eu/Eu [*] | 0.86 | 0.82 | 0.87 | 0.84 | 0.83 | 0.85 | 0.67 | 0.75 | 0.48 | 0.33 | 0.42 |
| (La/Yb) _N | 6.51 | 6.59 | 5.21 | 5.45 | 5.53 | 5.30 | 8.04 | 7.52 | 7.52 | 7.43 | 12.52 |
| (La/Gd) _N | 4.58 | 4.70 | 3.50 | 3.51 | 3.74 | 3.42 | 6.96 | 6.68 | 5.14 | 5.00 | 6.89 |
| (Gd/Yb) _N | 1.42 | 1.40 | 1.49 | 1.55 | 1.48 | 1.55 | 1.15 | 1.13 | 1.46 | 1.49 | 1.82 |
| Sc | 22.8 | 22.2 | 17.8 | 17.8 | 14.5 | 15.9 | 3.9 | 3.8 | 10.6 | 5.8 | 6.6 |
| V | 188.0 | 189.0 | 123.0 | 119.0 | 84.6 | 106.0 | 6.6 | 6.9 | 22.4 | 1.9 | 3.3 |
| Cr | 20.2 | 28.3 | 5.0 | 3.4 | 1.2 | 1.8 | 0.9 | 1.8 | 12.5 | 1.0 | 1.6 |
| Co | 22.3 | 22.4 | 15.8 | 15.2 | 10.1 | 12.0 | 1.3 | 1.0 | 0.9 | 0.3 | 0.2 |
| Ni | 8.4 | 12.3 | 3.5 | 3.3 | 1.8 | 2.8 | 1.0 | 0.6 | 2.1 | 0.5 | 0.6 |
| Ga | 18.1 | 17.9 | 20.3 | 19.2 | 18.2 | 19.1 | 17.1 | 17.4 | 21.5 | 21.6 | 17.0 |
| Rb | 45.9 | 34.9 | 90.8 | 101.0 | 69.1 | 78.9 | 124.0 | 99.7 | 185.0 | 204.0 | 189.0 |
| Sr | 357.0 | 356.0 | 393.0 | 348.0 | 375.0 | 580.0 | 128.0 | 176.0 | 12.9 | 9.3 | 11.6 |
| Y | 27.6 | 27.0 | 40.6 | 35.2 | 37.1 | 38.8 | 30.8 | 31.1 | 42.8 | 39.7 | 36.1 |
| Zr | 149.0 | 147.0 | 180.0 | 170.0 | 187.0 | 182.0 | 254.0 | 256.0 | 310.0 | 181.0 | 227.0 |
| Nb | 6.5 | 6.4 | 9.4 | 8.9 | 9.7 | 9.5 | 11.8 | 11.6 | 17.7 | 15.4 | 15.8 |
| Cs | 2.9 | 2.2 | 3.3 | 4.5 | 2.3 | 2.6 | 3.5 | 2.6 | 6.6 | 2.5 | 4.6 |
| Ba | 598.0 | 525.0 | 376.0 | 414.0 | 369.0 | 736.0 | 292.0 | 308.0 | 631.0 | 342.0 | 450.0 |
| Hf | 4.4 | 4.4 | 5.2 | 5.0 | 5.4 | 5.2 | 6.7 | 6.7 | 9.4 | 7.4 | 7.5 |
| Ta | 0.5 | 0.5 | 0.7 | 0.7 | 0.7 | 0.7 | 1.0 | 1.0 | 1.6 | 1.4 | 1.3 |
| Pb | 7.6 | 8.4 | 7.2 | 4.9 | 20.1 | 10.6 | 27.2 | 46.2 | 15.6 | 2.5 | 2.3 |
| Th | 8.6 | 8.4 | 8.7 | 8.0 | 9.2 | 8.6 | 16.3 | 15.9 | 31.3 | 35.4 | 25.1 |
| U | 1.0 | 1.0 | 1.5 | 1.4 | 1.6 | 1.5 | 2.7 | 2.6 | 4.5 | 2.9 | 3.5 |

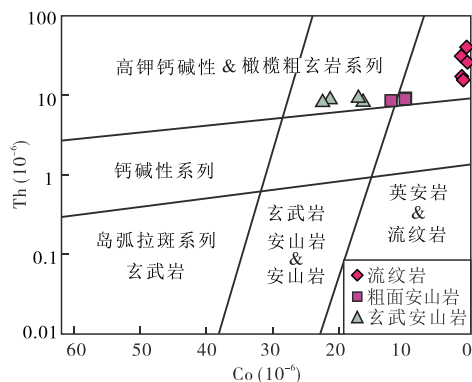


图 5 早白垩世火山岩的 Th-Co 关系

Fig.5 The relation of Th and Co for the Early Cretaceous volcanic rocks

据 Hastie *et al.*(2007)

弄群火山岩角度不整合覆盖于早二叠世拉嘎组和晚二叠世敌布错组之上,这种构造—地层关系指示该火山岩应代表则弄群火山岩的早期记录(朱弟成等,2008a),表明尼雄地区火山作用很可能开始于早白垩世。

近年来的研究表明,拉萨地块中北部普遍存在白垩纪则弄群火山岩,如位于格仁错南岸的尼阿节附近的则弄群火山岩获得了 113.6 ± 1.1 Ma 的锆石 U-Pb 年龄(康志强等,2008);位于拉萨地体中北部的措勤地区也报道了 $130 \sim 110$ Ma 的则弄群火山岩(朱弟成等,2008a; 刘伟等,2010);而西藏改则县错果错地区则弄群火山岩形成于 143 Ma(张志平等,2016)。结合区域上发现的大量白垩纪岩浆岩,如西藏措勤麦嘎岩基($122 \sim 113$ Ma; 张晓倩等,2012)、措勤地区达雄花岗闪长岩(107 Ma; 周长勇等,2008)、尼雄滚纠花岗闪长岩和二长花岗岩(113 Ma; 于玉帅等,2011)等,以及区域上桑日群的

出现(主体以晚侏罗世—早白垩世形成的岛弧钙碱性—拉斑系列的火山—沉积为主; 莫宣学和潘桂棠,2006),笔者认为拉萨地块经历了强烈的早白垩世火山—岩浆作用,这一观点也得到了中部拉萨地块中北部地区则弄群火山岩可能开始于约 130 Ma、结束于约 110 Ma 的进一步佐证(朱弟成等,2008a)。

5.2 岩石成因

岩石化学分析结果表明,研究区玄武安山岩、粗面安山岩和流纹岩均为铁质—镁质、钙性—碱钙性岩石(图 7a, 7b; Frost and Frost, 2010)。这些岩石具有较高的 SiO_2 含量($55.76\% \sim 78.78\%$), 相对较低的 $\text{Mg}^{\#}$ (最大值仅为 49.26, 平均值为 38.39), 不可能通过地幔岩部分直接熔融生成(Baker *et al.*, 1995)。尽管它们的 Th/U 值($5.66 \sim 12.21$)、Nb/Ta 值($10.77 \sim 14.06$)和 Th 值($8.0 \times 10^{-6} \sim 35.4 \times 10^{-6}$)均与大陆地壳的 Th/U 值(6; Rudnick and Gao, 2003)、Nb/Ta 值($12 \sim 13$; Barth *et al.*, 2000)和 Th 值($6.5 \times 10^{-6} \sim 10.5 \times 10^{-6}$; Rudnick and Gao, 2003)部分重合,并具有与陆壳非常相似的蛛网图(图 6a)。然而,基性下地壳部分熔融形成的岩石往往具有低的 $\text{Mg}^{\#}$ 值(<40)和低的 MgO 含量(大多 $<1\%$; Rapp and Watson, 1995; 丁慧霞等, 2015),而研究区玄武安山岩和粗面安山岩的 MgO 含量(分别为 $>3\%$ 和 $>2.5\%$)明显偏高,表明其并非全部由下地壳部分熔融形成。此外,则弄群火山岩的 $\epsilon_{\text{Nd}}(t)$ 变化范围较大($-3.4 \sim -9.3$; 刘伟等, 2010),表明这些火山岩很可能是壳幔熔体混合的结果。而同期的拉萨地块中北部花岗岩类具有跨度大的 $\epsilon_{\text{Nd}}(t)$ 值($-5.3 \sim -17.3$; 莫宣学等, 2006),并在其中常见大量的长英质包体,也进一步说明了则弄

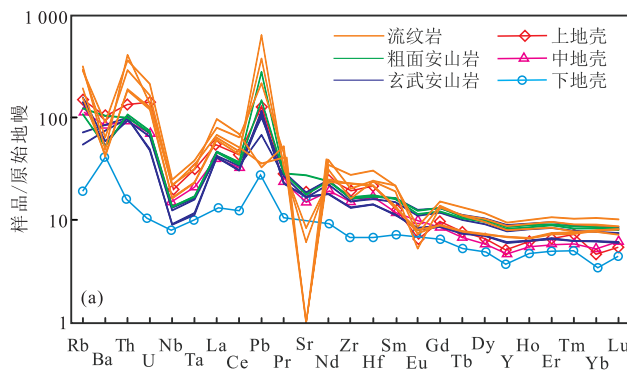
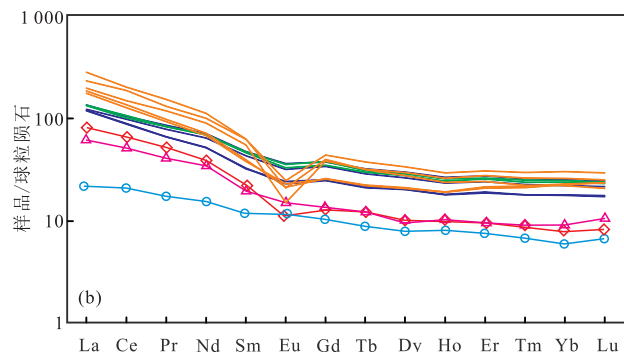


图 6 早白垩世火山岩原始地幔标准化微量元素蛛网图(a)及球粒陨石标准化稀土元素配分模式(b)

Fig.6 Primitive-mantle-normalized trace element spider diagram (a) and chondrite-normalized REE pattern (b) of the Early Cretaceous volcanic rocks

标准值据 Sun and McDonough (1989); 上、中、下地壳值据 Rudnick and Gao(2003)



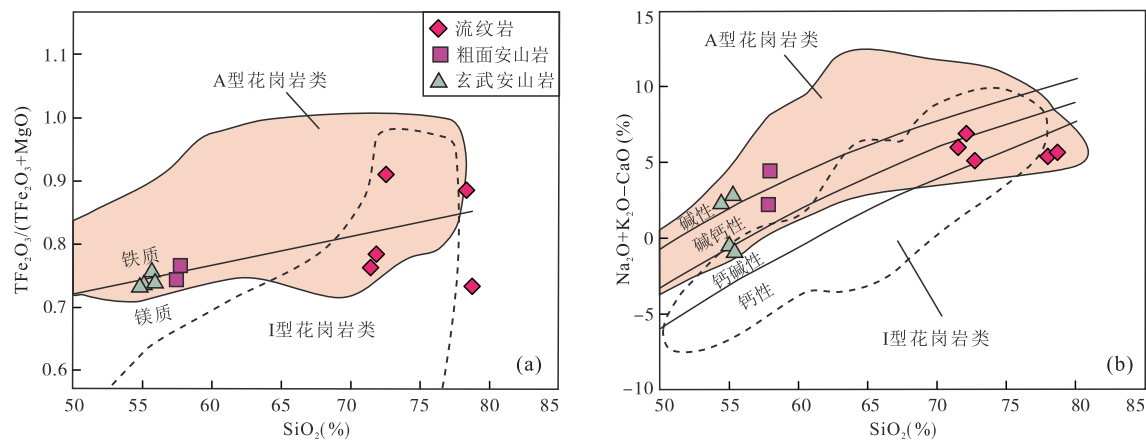


图 7 早白垩世火山岩 $T\text{Fe}_2\text{O}_3/(T\text{Fe}_2\text{O}_3+\text{MgO})-\text{SiO}_2$ 图解(a)与 $(\text{Na}_2\text{O}+\text{K}_2\text{O}-\text{CaO})-\text{SiO}_2$ 图解(b)

Fig.7 Plots of $T\text{Fe}_2\text{O}_3/(T\text{Fe}_2\text{O}_3+\text{MgO})$ vs. SiO_2 (a) and $(\text{Na}_2\text{O}+\text{K}_2\text{O}-\text{CaO})$ vs. SiO_2 (b) of the Early Cretaceous volcanic rocks

图 a 修改自 Frost *et al.* (2001) 和 Rajesh (2007); 图 b 据 Frost *et al.* (2001)

群火山岩很可能来自一个壳幔混合的源区。

此外,研究区流纹岩样品具有较高的 SiO_2 含量(71.36%~78.78%)和较低的 MgO (0.26%~0.66%)、 TiO_2 (0.11%~0.36%)、 P_2O_5 (0.03%~0.09%)含量和 δEu 值(0.33~0.75)。在微量元素蛛网图和稀土元素配分曲线上,流纹岩样品显示出明显 Ba 、 Sr 、 Eu 、 Nb 、 Ta 的负异常(图 6a, 6b),表明其可能经历了斜长石结晶分离作用。

5.3 构造背景

研究区则弄群火山岩富集 Th 、 U 、 Pb 等元素,亏损 Nb 、 Ta 等高场强元素(图 6a),显示出岛弧岩浆岩的特征(McCulloch and Gamble, 1991)。此外,所研究的火山岩均具有较高的 $(\text{La}/\text{Nb})_N$ 值(3.09~4.51),与岛弧岩浆岩的特征一致(>1 ; Kerr *et al.*, 2000)。在图 8 中,研究区则弄群火山岩样品均投点于火山弧区域,表现出弧岩浆岩的亲缘性。与此同时,研究区还发育一套与则弄群火山岩在时间、空间和成因上都具有紧密联系的侵入岩组合(二长花岗岩—花岗闪长岩系列),而这些侵入岩均被证实属钙碱性岩石,并具有典型的弧岩浆岩特征(于玉帅等,2011;张晓倩等,2012)。同时,张志平等(2016)在研究区及邻区零星出露的凝灰岩中发现了植物碎片,也暗示了早白垩世则弄群火山活动发生于岛弧环境。考虑到拉萨地块中北部在早白垩世出现的大规模火山—岩浆作用,以及幔源热物质加入(Zhu *et al.*, 2009b, 2011)等事实,笔者推测拉萨地块中北部在早白垩世晚期可能经历了俯冲洋壳板片断离、回转,并伴随有幔源热加入导致地壳重熔的事件

发生(隋清霖, 2014)。

目前对于在拉萨地块中北部大规模出露的早白垩世火山岩的构造环境,学者们存在着不同认识。朱弟成等(2006)认为拉萨地体中北部早白垩世的火山岩是班公—怒江洋壳南向俯冲消减的产物,与新特提斯洋壳北向俯冲关系不大,其主要证据是,拉萨地块晚侏罗世—早白垩世火山岩岩石系列从北向南依次由中钾钙碱系列向高钾钙碱性系列过渡变化。而基于拉萨地体与羌塘地体碰撞时间与板片断离的时空联系,Zhang *et al.*(2012)认为拉萨地体中北部普遍发育的白垩纪(135~100 Ma)火山—岩浆作用与新特提斯洋壳向北俯冲有关。朱同兴等(2006)的研究也表明,早期与新特提斯洋连接的印度岩石圈在白垩纪时期已经俯冲到拉萨地块的北部甚至班公湖—怒江缝合带(Barazangi and Ni, 1982)。上述 2 种模型均可导致俯冲的板片断离并发生回转,从而引起软流圈物质上涌,并诱发古老地壳脱水发生重熔,进而形成中酸性岛弧型岩浆岩。因此,笔者倾向于认为拉萨地体中北部则弄群火山岩可能同时遭受新特提斯洋壳北向俯冲和班公湖—怒江洋壳南向俯冲的共同影响。其他证据如下:(1)尼雄地区发现的早白垩世火山岩处于冈底斯弧背断隆带内,构造上介于雅鲁藏布江缝合带和班公湖—怒江缝合带之间(图 1a),距离二者的距离均为 200 多千米,可以同时受到二者俯冲作用的影响。(2)从拉萨地块中北部的则弄群火山岩到中拉萨地体白垩纪则弄群和多尼组火山岩均显示出,从北到南,岩性组合由中钾钙碱系列逐渐变化为高钾钙碱性系列,其形成年龄由北

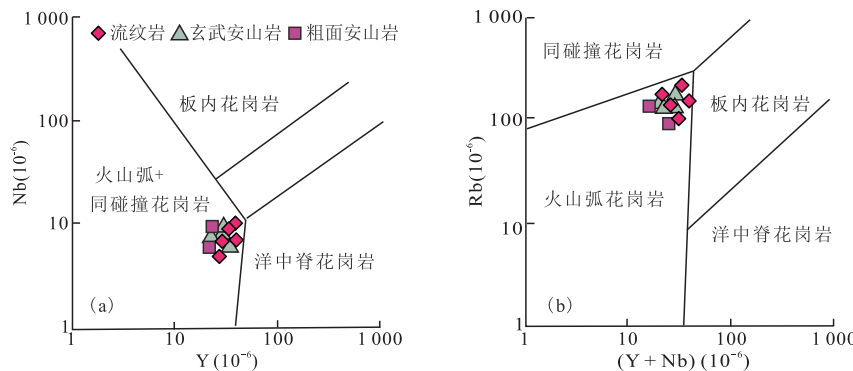


图 8 早白垩世火山岩 Nb—Y(a) 和 Rb—(Y+Nb)(b) 判别图解

Fig.8 Nb vs. Y (a) and Rb vs. (Y+Nb) (b) discrimination diagrams of the Early Cretaceous volcanic rocks

据 Pearce and Norry (1979)

部到中部有逐渐变新的趋势,这些分布特点指示了俯冲带深度由北部向中部逐渐变深,俯冲极性从北到南(马国林和岳雅慧,2010;王力圆等,2016);然而,从南冈底斯带的火山岩到中拉萨地块的白垩纪火山岩,其岩性组合由拉斑系列—钙碱性系列逐渐过渡为高钾钙碱性、甚至钾玄质系列,且其形成年龄也有由老变新的趋势,指示俯冲带深度由南向中部逐渐变深,俯冲极性由南向北。因此,上述特征暗示了拉萨地块在早白垩世时期,可能同时受到双向俯冲的制约。(3)考虑到导致雅鲁藏布新特提斯洋开启及向北俯冲的动力学机制可能来源于班公湖—怒江洋壳岩石圈向南、雅鲁藏布江新特提斯洋壳岩石圈向北双向俯冲的影响。

总之,基于详细的地质观察以及上述火山岩地球化学、年代学分析,笔者倾向于认为拉萨地体中北部在早白垩世很可能既受到了新特提斯洋壳沿拉萨地体南缘北向俯冲的影响,也受到了班公—怒江特提斯洋壳沿拉萨地体北缘南向俯冲的制约。

6 结论

(1)拉萨地块中北部尼雄地区普遍发育早白垩纪的玄武安山岩、粗面安山岩和流纹岩,其结晶年龄为 117~127 Ma,被重新厘定为早白垩世则弄群,否定了前人归属为渐新世日贡拉组(E_3r)及始新世年波组(E_2n)的认识。

(2)尼雄地区则弄群火山岩属中—高钾钙碱性岩

石,表现出弧岩浆岩的特征,其可能为壳幔熔体混合的结果。流纹岩母岩浆形成后又遭受了结晶分离作用。

(3)尼雄地区则弄群火山岩可能同时受到班公湖—怒江洋壳岩石圈向南、雅鲁藏布江新特提斯洋壳岩石圈向北双向俯冲的影响。

致谢:贵州地质调查院的领导和同仁在野外地质调查期间提供了大力帮助,在成文过程中得到了李奋其研究员的指点,3位审稿专家及编辑部提出许多建设性的意见和建议,在此一并表示感谢!

References

- Baker, M.B., Hirschmann, M.M., Ghiorso, M.S., et al., 1995. Compositions of Near-Solidus Peridotite Melts from Experiments and Thermodynamic Calculations. *Nature*, 375 (6529): 308—311. <https://doi.org/10.1038/375308a0>
- Barazangi, M., Ni, J., 1982. Velocities and Propagation Characteristics of Pn and Sn beneath the Himalayan Arc and Tibetan Plateau: Possible Evidence for Underthrusting of Indian Continental Lithosphere beneath Tibet. *Geology*, 10 (4): 179—185. [https://doi.org/10.1130/0091-7613\(1982\)10<179:vacop>2.0.co;2](https://doi.org/10.1130/0091-7613(1982)10<179:vacop>2.0.co;2)
- Barth, M.G., McDonough, W.F., Rudnick, R.L., 2000. Tracking the Budget of Nb and Ta in the Continental Crust. *Chemical Geology*, 165 (3—4): 197—213. [https://doi.org/10.1016/s0009-2541\(99\)00173-4](https://doi.org/10.1016/s0009-2541(99)00173-4)
- Chang, C.F., Zheng, X.L., 1973. Discussion on the Formation of Western-Eastern Ranges in Himalayas and Qinghai-Xizang Plateau and Characteristics of Geological Structure in Everest Region. *Science in China (Series D)*, 2: 190—201 (in Chinese).
- Chen, Y., Zhu, D.C., Zhao, Z.D., et al., 2014. Slab Break off Triggered ca. 113 Ma Magmatism around Xainza Area of the

- Lhasa Terrane, Tibet. *Gondwana Research*, 26(2): 449—463. <https://doi.org/10.1016/j.gr.2013.06.005>
- Chung, S.L., Chu, M.F., Ji, J.Q., et al., 2009. The Nature and Timing of Crustal Thickening in Southern Tibet: Geochemical and Zircon Hf Isotopic Constraints from Post-collisional Adakites. *Tectonophysics*, 477 (1—2): 36—48. <https://doi.org/10.1016/j.tecto.2009.08.008>
- Ding, H.X., Zhang, Z.M., Xiang, H., et al., 2015. The Petrogenesis and Tectonic Significance of the Early Cretaceous Volcanics from the Northern Lhasa Terrane, Tibet. *Acta Petrologica Sinica*, 31(5): 1247—1267 (in Chinese with English abstract).
- Dong, X., Zhang, Z.M., Santosh, M., et al., 2011. Late Neoproterozoic Thermal Events in the Northern Lhasa Terrane, South Tibet: Zircon Chronology and Tectonic Implications. *Journal of Geodynamics*, 52(5): 389—405. <https://doi.org/10.1016/j.jog.2011.05.002>
- Frost, B.R., Barnes, C.G., Collins, W.J., et al., 2001. A Geochemical Classification for Granitic Rocks. *Journal of Petrology*, 42(11): 2033—2048. <https://doi.org/10.1093/petrology/42.11.2033>
- Frost, C.D., Frost, B.R., 2010. On Ferroan (A-Type) Granitoids: Their Compositional Variability and Modes of Origin. *Journal of Petrology*, 52(1): 39—53. <https://doi.org/10.1093/petrology/egq070>
- Guan, Q., Zhu, D.C., Zhao, Z.D., et al., 2010. Late Cretaceous Adakites from the Eastern Segment of the Gangdese Belt, Southern Tibet: Products of Neo-Tethyan Mid-Ocean Ridge Subduction? *Acta Petrologica Sinica*, 26(7): 2165—2179 (in Chinese with English abstract).
- Guo, L., Zhang, H. F., Harris, N., et al., 2012. Paleogene Crustal Anatexis and Metamorphism in Lhasa Terrane, Eastern Himalayan Syntaxis: Evidence from U-Pb Zircon Ages and Hf Isotopic Compositions of the Nyingschi Complex. *Gondwana Research*, 21(1): 100—111. <https://doi.org/10.1016/j.gr.2011.03.002>
- Harris, N.B.W., Inger, S., Xu, R.H., 1990. Cretaceous Plutonism in Central Tibet: An Example of Post-Collision Magmatism? *Journal of Volcanology and Geothermal Research*, 44(1—2): 21—32. [https://doi.org/10.1016/0377-0273\(90\)90009-5](https://doi.org/10.1016/0377-0273(90)90009-5)
- Hastie, A.R., Kerr, A.C., Pearce, J.A., et al., 2007. Classification of Altered Volcanic Island Arc Rocks Using Immobile Trace Elements: Development of the Th-Co Discrimination Diagram. *Journal of Petrology*, 48(12): 2341—2357. <https://doi.org/10.1093/petrology/egm062>
- Hoskin, P.W.O., Schaltegger, U., 2003. The Composition of Zircon and Igneous and Metamorphic Petrogenesis. *Reviews in Mineralogy and Geochemistry*, 53(1): 27—62. <https://doi.org/10.2113/0530027>
- Kang, Z.Q., Xu, J.F., Dong, Y.H., et al., 2008. Cretaceous Volcanic Rocks of Zenong Group in North-Middle Lhasa Block: Products of Southward Subducting of the Slainajap Ocean? *Acta Petrologica Sinica*, 24(2): 303—314 (in Chinese with English abstract).
- Kang, Z.Q., Xu, J.F., Wang, B.D., et al., 2009. Geochemistry of Cretaceous Volcanic Rocks of Duoni Formation in Northern Lhasa Block: Discussion of Tectonic Setting. *Earth Science*, 34(1): 89—104 (in Chinese with English abstract).
- Kapp, P., Yin, A., Harrison, T.M., et al., 2005. Cretaceous-Tertiary Shortening, Basin Development, and Volcanism in Central Tibet. *Geological Society of America Bulletin*, 117(7): 865—878. <https://doi.org/10.1130/b25595.1>
- Kerr, A.C., White, R.V., Saunders, A.D., 2000. LIP Reading: Recognizing Oceanic Plateaux in the Geological Record. *Journal of Petrology*, 41(7): 1041—1056. <https://doi.org/10.1093/petrology/41.7.1041>
- Li, C., Wang, T.W., Li, H.M., et al., 2003. Discovery of Indosian Megaporphyritic Granodiorite in the Gangdese Area: Evidence for the Existence of Paleo-Gangdese. *Geological Bulletin of China*, 22(5): 364—366 (in Chinese with English abstract).
- Liang, Y.P., Zhu, J., Ci, Q., et al., 2010. Zircon U-Pb Ages and Geochemistry of Volcanic Rock from Linzizong Group in Zhunuo Area in Middle Gangdise Belt, Tibet Plateau. *Earth Science*, 35(2): 211—223 (in Chinese with English abstract). <https://doi.org/10.3799/dqkx.2010.021>
- Lin, Y.H., Zhang, Z.M., Dong, X., et al., 2013. Precambrian Evolution of the Lhasa Terrane, Tibet: Constraint from the Zircon U-Pb Geochronology of the Gneisses. *Precambrian Research*, 237: 64—77. <https://doi.org/10.1016/j.precamres.2013.09.006>
- Liu, W., Li, F.Q., Yuan, S.H., et al., 2010. Volcanic Rock Provenance of Zenong Group in Coqen Area of Tibet: Geochemistry and Sr-Nd Isotopic Constraint. *Acta Petrologica et Mineralogica*, 29(4): 367—376 (in Chinese with English abstract).
- Liu, Y.S., Hu, Z.C., Zong, K.Q., et al., 2010. Reappraisal and Refinement of Zircon U-Pb Isotope and Trace Element Analyses by LA-ICP-MS. *Chinese Science Bulletin*, 55(15): 1535—1546. <https://doi.org/10.1007/s11434-010-3052-4>
- Ludwig, K.R., 2003. Isoplot/Ex Version 3.00: A Geochronological Toolkit for Microsoft Excel. Berkeley Geochronology Center Special Publication, Berkeley.
- Ma, G.L., Yue, Y.H., 2010. Cretaceous Volcanic Rocks in

- Northern Lhasa Block: Constraints on the Tectonic Evolution of the Gangdise Arc. *Acta Petrologica et Mineralogica*, 29(5):525–538 (in Chinese with English abstract).
- Ma, L., Wang, Q., Li, Z.X., et al., 2013. Early Late Cretaceous (ca. 93 Ma) Norites and Hornblendites in the Milin Area, Eastern Gangdese: Lithosphere-Asthenosphere Interaction during Slab Roll-Back and an Insight into Early Late Cretaceous (ca. 100 – 80 Ma) Magmatic “Flare-Up” in Southern Lhasa (Tibet). *Lithos*, 172 – 173:17 – 30. <https://doi.org/10.13039/501100002367>
- McCulloch, M.T., Gamble, J.A., 1991. Geochemical and Geodynamical Constraints on Subduction Zone Magmatism. *Earth and Planetary Science Letters*, 102(3–4):358 – 374. [https://doi.org/10.1016/0012-821x\(91\)90029-h](https://doi.org/10.1016/0012-821x(91)90029-h)
- Meng, F.Y., Zhao, Z.D., Zhu, D.C., et al., 2014. Late Cretaceous Magmatism in Mamba Area, Central Lhasa Subterrane: Products of Back-Arc Extension of Neo-Tethyan Ocean? *Gondwana Research*, 26 (2): 505 – 520. <https://doi.org/10.1016/j.gr.2013.07.017>
- Mo, X.X., Niu, Y.L., Dong, G.C., et al., 2008. Contribution of Syncollisional Felsic Magmatism to Continental Crust Growth: A Case Study of the Paleogene Linzizong Volcanic Succession in Southern Tibet. *Chemical Geology*, 250(1 – 4):49 – 67. <https://doi.org/10.1016/j.chemgeo.2008.02.003>
- Mo, X.X., Pan, G.T., 2006. From the Tethys to the Formation of the Qinghai-Tibet Plateau: Constrained by Tectonic-Magmatic Events. *Earth Science Frontiers*, 13 (6):43 – 51 (in Chinese with English abstract).
- Mo, X.X., Zhao, Z.D., DePaolo, D.J., et al., 2006. Three Types of Collisional and Post-Collisional Magmatism in the Lhasa Block, Tibet and Implications for India Intracontinental Subduction and Mineralization: Evidence from Sr-Nd Isotopes. *Acta Petrologica Sinica*, 22(4):795 – 803 (in Chinese with English abstract).
- Pan, G. T., Ding, J., Yao, D. S., et al., 2004. Guidebook of 1 : 1 500 000 Geologic Map of the Qinghai-Xizang (Tibet) Plateau and Adjacent Areas. Chengdu, Chengdu Cartographic Publishing House.
- Pearce, J.A., Norry, M.J., 1979. Petrogenetic Implications of Ti, Zr, Y, and Nb Variations in Volcanic Rocks. *Contributions to Mineralogy and Petrology*, 69(1):33 – 47. <https://doi.org/10.1007/bf00375192>
- Rajesh, H.M., 2007. The Petrogenetic Characterization of Intermediate and Silicic Charnockites in High-Grade Terrains: A Case Study from Southern India. *Contributions to Mineralogy and Petrology*, 154 (5): 591 – 606. <https://doi.org/10.1007/s00410-007-0211-y>
- Rapp, R.P., Watson, E.B., 1995. Dehydration Melting of Metabasalt at 8 – 32 Kbar: Implications for Continental Growth and Crust-Mantle Recycling. *Journal of Petrology*, 36(4):891 – 931. <https://doi.org/10.1093/petrology/36.4.891>
- Rubatto, D., Scambelluri, M., 2003. U-Pb Dating of Magmatic Zircon and Metamorphic Baddeleyite in the Ligurian Eclogites (Voltri Massif, Western Alps). *Contributions to Mineralogy and Petrology*, 146 (3): 341 – 355. <https://doi.org/10.1007/s00410-003-0502-x>
- Rudnick, R.L., Gao, S., 2003. Composition of the Continental Crust. In: Rudnick, R. L., ed., *The Crust: Treaties on Geochemistry*. Elsevier Pergamon, Oxford.
- Sui, Q. L., 2014. The Geochronology, Petrogenesis and Tectonic Significance of the Early Cretaceous Magmatic Rocks from Yanhu, the Lhasa Terrane, Tibet (Dissertation). China University of Geosciences, Beijing (in Chinese with English abstract).
- Sun, S. S., McDonough, W. F., 1989. Chemical and Isotopic Systematics of Oceanic Basalts: Implications for Mantle Composition and Processes. *Geological Society, London, Special Publications*, 42 (1): 313 – 345. <https://doi.org/10.1144/gsl.sp.1989.042.01.19>
- Wang, L.Y., Zheng, Y.Y., Gao, S.B., et al., 2016. The Discovery of the Early Cretaceous Zenong Group Volcanic Rocks and Geological Significance in Jiwa Area in South of the Central Lhasa Subterrane. *Acta Petrologica Sinica*, 32(5):1543 – 1555 (in Chinese with English abstract).
- Whalen, J. B., Currie, K. L., Chappell, B. W., 1987. A-Type Granites: Geochemical Characteristics, Discrimination and Petrogenesis. *Contributions to Mineralogy and Petrology*, 95 (4): 407 – 419. <https://doi.org/10.1007/bf0042202>
- Winchester, J.A., Floyd, P.A., 1977. Geochemical Discrimination of Different Magma Series and Their Differentiation Products Using Immobile Elements. *Chemical Geology*, 20 (4): 325 – 343. [https://doi.org/10.1016/0009-2541\(77\)90057-2](https://doi.org/10.1016/0009-2541(77)90057-2)
- Wu, Y.B., Zheng, Y.F., 2004. Genesis of Zircon and Its Constraints on Interpretation of U-Pb Age. *Chinese Science Bulletin*, 49(16):1589 – 1604 (in Chinese).
- Xu, W.C., Zhang, H.F., Harris, N., et al., 2013. Geochronology and Geochemistry of Mesoproterozoic Granitoids in the Lhasa Terrane, South Tibet: Implications for the Early Evolution of Lhasa Terrane. *Precambrian Research*, 236(5):46 – 58. <https://doi.org/10.1016/j.precambrian.2013.09.011>

- camres.2013.07.016
- Yin, A., Harrison, T.M., 2000. Geologic Evolution of the Himalayan-Tibetan Orogen. *Annual Review of Earth and Planetary Sciences*, 28(1): 211—280. <https://doi.org/10.1146/annurev.earth.28.1.211>
- Yu, Y.S., Gao, Y., Yang, Z.S., et al., 2011. Zircon LA-ICP-MS U-Pb Dating and Geochemistry of Intrusive Rocks from Gunjiu Iron Deposit in the Nixiong Ore Field, Coqen, Tibet. *Acta Petrologica Sinica*, 27(7): 1949—1960 (in Chinese with English abstract).
- Zhang, K.J., Zhang, Y.X., Tang, X.C., et al., 2012. Late Mesozoic Tectonic Evolution and Growth of the Tibetan Plateau Prior to the Indo-Asian Collision. *Earth-Science Reviews*, 114 (3—4): 236—249. <https://doi.org/10.1016/j.earscirev.2012.06.001>
- Zhang, L.L., Zhu, D.C., Zhao, Z.D., et al., 2010. Petrogenesis of Magmatism in the Baerda Region of Northern Gangdese, Tibet: Constraints from Geochemistry, Geochronology and Sr-Nd-Hf Isotopes. *Acta Petrologica Sinica*, 26(6): 1871—1888 (in Chinese with English abstract).
- Zhang, X.Q., Zhu, D.C., Zhao, Z.D., et al., 2012. Geochemistry, Zircon U-Pb Geochronology and In-Situ Hf Isotope of the Maiga Batholith in Coqen, Tibet; Constraints on the Petrogenesis of the Early Cretaceous Granitoids in the Central Lhasa Terrane. *Acta Petrologica Sinica*, 28 (5): 1615—1634 (in Chinese with English abstract).
- Zhang, Z.M., Zhao, G.C., Santosh, M., et al., 2010. Late Cretaceous Charnockite with Adakitic Affinities from the Gangdese Batholith, Southeastern Tibet: Evidence for Neo-Tethyan Mid-Ocean Ridge Subduction? *Gondwana Research*, 17(4): 615—631. <https://doi.org/10.1016/j.gr.2009.10.007>
- Zhang, Z.P., Dong, H., Wu, Y., et al., 2016. Geochemical Characteristics and Tectonic Significance of Zenong Group Volcanic Rocks in Cuoguoqo Area of Gaize, Tibet. *Gansu Geology*, 25(4): 22—28 (in Chinese with English abstract).
- Zheng, X.S., Sang, H.Q., Qiu, J., et al., 2010. New Discovery of the Early Cretaceous Volcanic Rocks on the Barton Peninsula, King George Island, Antarctica and Its Geological Significance. *Acta Geologica Sinica (English Edition)*, 74(2): 176—182. <https://doi.org/10.1111/j.1755-6724.2000.tb00446.x>
- Zhou, C.Y., Zhu, D.C., Zhao, Z.D., et al., 2008. Petrogenesis of Daxiong Pluton in Western Gangdese, Tibet: Zircon U-Pb Dating and Hf Isotopic Constraints. *Acta Petrologica Sinica*, 24(2): 348—358 (in Chinese with English abstract).
- Zhu, D.C., Mo, X.X., Zhao, Z.D., et al., 2008a. Zircon U-Pb Geochronology of Zenong Group Volcanic Rocks in Coqen Area of the Gangdese, Tibet and Tectonic Significance. *Acta Petrologica Sinica*, 24 (3): 401—412 (in Chinese with English abstract).
- Zhu, D.C., Mo, X.X., Wang, L.Q., et al., 2008b. Hotspot-Ridge Interaction for the Evolution of Neo-Tethys: Insights from the Late Jurassic-Early Cretaceous Magmatism in Southern Tibet. *Acta Petrologica Sinica*, 24 (2): 225—237 (in Chinese with English abstract).
- Zhu, D.C., Mo, X.X., Zhao, Z.D., 2009. Permian and Early Cretaceous Tectonomagmatism in Southern Tibet and Tethyan Evolution: New Perspective. *Earth Science Frontiers*, 16 (2): 1—20 (in Chinese with English abstract).
- Zhu, D.C., Pan, G.T., Chung, S.L., et al., 2008. SHRIMP Zircon Age and Geochemical Constraints on the Origin of Lower Jurassic Volcanic Rocks from the Yeba Formation, Southern Gangdese, South Tibet. *International Geology Review*, 50 (5): 442—471. <https://doi.org/10.2747/0020-6814.50.5.442>
- Zhu, D.C., Pan, G.T., Mo, X.X., et al., 2006. Late Jurassic-Early Cretaceous Geodynamic Setting in Middle-Northern Gangdese: New Insights from Volcanic Rocks. *Acta Petrologica Sinica*, 22(3): 536—546 (in Chinese with English abstract).
- Zhu, D.C., Zhao, Z.D., Niu, Y.L., et al., 2011. The Lhasa Terrane: Record of a Microcontinent and Its Histories of Drift and Growth. *Earth and Planetary Science Letters*, 301(1—2): 241—255. <https://doi.org/10.13039/501100001809>
- Zhu, D.C., Zhao, Z.D., Niu, Y.L., et al., 2012. Cambrian Bimodal Volcanism in the Lhasa Terrane, Southern Tibet: Record of an Early Paleozoic Andean-Type Magmatic Arc in the Australian Proto-Tethyan Margin. *Chemical Geology*, 328 (11): 290—308. <https://doi.org/10.1016/j.chemgeo.2011.12.024>
- Zhu, D.C., Zhao, Z.D., Pan, G.T., et al., 2009a. Early Cretaceous Subduction-Related Adakite-Like Rocks of the Gangdese Belt, Southern Tibet: Products of Slab Melting and Subsequent Melt-Peridotite Interaction? *Journal of Asian Earth Sciences*, 34(3): 298—309. <https://doi.org/10.1016/j.jseas.2008.05.003>
- Zhu, D.C., Mo, X.X., Niu, Y.L., et al., 2009b. Geochemical Investigation of Early Cretaceous Igneous Rocks along an East-West Traverse throughout the Central Lhasa Terrane, Tibet. *Chemical Geology*, 268 (3—4): 298—312. <https://doi.org/10.13039/50110002858>
- Zhu, T.X., Zhuang, Z.H., Zhou, M.K., et al., 2006. New Ordovi-

cian-Paleogene Tectonomagnetic Data from the Northern Slope of the Himalayas. *Geological Bulletin of China*, 25 (1-2): 76-82 (in Chinese with English abstract).

附中文参考文献

- 常承法, 郑锡澜, 1973. 中国西藏南部珠穆朗玛地区地质构造特征及其青藏高原东西向诸山系形成的探讨. 中国科学(D辑), 2: 190-201.
- 丁慧霞, 张泽明, 向华, 等, 2015. 青藏高原拉萨地体北部早白垩世火山岩的成因及意义. 岩石学报, 31(5): 1247-1267.
- 管琪, 朱弟成, 赵志丹, 等, 2010. 西藏南部冈底斯带东段晚白垩世埃达克岩: 新特提斯洋脊俯冲的产物? 岩石学报, 26(7): 2165-2179.
- 康志强, 许继峰, 董彦辉, 等, 2008. 拉萨地块中北部白垩纪则弄群火山岩: Slainajap 洋南向俯冲的产物? 岩石学报, 24(2): 303-314.
- 康志强, 许继峰, 王保弟, 等, 2009. 拉萨地块北部白垩纪多尼组火山岩的地球化学: 形成的构造环境. 地球科学, 34 (1): 89-104.
- 李才, 王天武, 李惠民, 等, 2003. 冈底斯地区发现印支期巨斑花岗闪长岩: 古冈底斯造山的存在证据. 地质通报, 22 (5): 364-366.
- 刘伟, 李奋其, 袁四化, 等, 2010. 西藏措勤地区则弄群火山岩源区—地球化学及 Sr-Nd 同位素制约. 岩石矿物学杂志, 29(4): 367-376.
- 梁银平, 朱杰, 次邛, 等, 2010. 青藏高原冈底斯带中部朱诺地区林子宗群火山岩锆石 U-Pb 年龄和地球化学特征. 地球科学, 35(2): 211-223. <https://doi.org/10.3799/dqkx.2010.021>
- 马国林, 岳雅慧, 2010. 西藏拉萨地块北部白垩纪火山岩及其对冈底斯岛弧构造演化的制约. 岩石矿物学杂志, 29 (5): 525-538.
- 莫宣学, 潘桂棠, 2006. 从特提斯到青藏高原形成: 构造—岩浆事件的约束. 地学前缘, 13(6): 43-51.
- 莫宣学, 赵志丹, Depaolo, D.J., 等, 2006. 青藏高原拉萨地块碰撞—后碰撞岩浆作用的三种类型及其对大陆俯冲和成矿作用的启示: Sr-Nd 同位素证据. 岩石学报, 22(4): 795-803.
- 隋清霖, 2014. 西藏拉萨地块盐湖地区早白垩世岩浆岩年代学、岩石成因及构造意义(硕士学位论文). 北京: 中国地质大学.
- 王力圆, 郑有业, 高顺宝, 等, 2016. 中部拉萨地体南侧吉瓦地区早白垩世则弄群火山岩的发现及意义. 岩石学报, 32 (5): 1543-1555.
- 吴元保, 郑永飞, 2004. 锆石成因矿物学研究及其对 U-Pb 年龄解释的制约. 科学通报, 49(16): 1589-1604.
- 于玉帅, 高原, 杨竹森, 等, 2011. 西藏措勤尼雄矿田滚纠铁矿侵入岩 LA-ICP-MS 锆石 U-Pb 年龄与地球化学特征. 岩石学报, 27(7): 1949-1960.
- 张亮亮, 朱弟成, 赵志丹, 等, 2010. 西藏北冈底斯巴尔达地区岩浆作用的成因: 地球化学、年代学及 Sr-Nd-Hf 同位素约束. 岩石学报, 26(6): 1871-1888.
- 张晓倩, 朱弟成, 赵志丹, 等, 2012. 西藏措勤麦嘎岩基的锆石 U-Pb 年代学、地球化学和锆石 Hf 同位素: 对中部拉萨地块早白垩世花岗岩类岩石成因的约束. 岩石学报, 28 (5): 1615-1634.
- 张志平, 董瀚, 吴勇, 等, 2016. 西藏改则县错果错地区则弄群火山岩岩石地球化学特征及其构造意义. 甘肃地质, 25 (4): 22-28.
- 周长勇, 朱弟成, 赵志丹, 等, 2008. 西藏冈底斯带西部达雄岩体的岩石成因: 锆石 U-Pb 年龄和 Hf 同位素约束. 岩石学报, 24(2): 348-358.
- 朱弟成, 莫宣学, 赵志丹, 等, 2008a. 西藏冈底斯带措勤地区则弄群火山岩锆石 U-Pb 年代学格架及构造意义. 岩石学报, 24(3): 401-412.
- 朱弟成, 莫宣学, 王立全, 等, 2008b. 新特提斯新特提斯演化的热点与洋脊相互作用: 西藏南部晚侏罗世—早白垩世岩浆作用推论. 岩石学报, 24(2): 225-237.
- 朱弟成, 莫宣学, 赵志丹, 等, 2009. 西藏南部二叠纪和早白垩世构造岩浆作用与特提斯演化: 新观点. 地学前缘, 16 (2): 1-20.
- 朱弟成, 潘桂棠, 莫宣学, 等, 2006. 冈底斯中北部晚侏罗世—早白垩世地球动力学环境: 火山岩约束. 岩石学报, 22 (3): 534-546.
- 朱同兴, 庄忠海, 周铭魁, 等, 2006. 喜马拉雅山北坡奥陶纪—古近纪构造古地磁新数据. 地质通报, 25(1-2): 76-82.